



**HAL**  
open science

# Impact of different activation wavefronts on ischemic myocardial scar electrophysiological properties during high-density ventricular tachycardia mapping and ablation

Gustavo Lima da Silva, Nuno Cortez-dias, Afonso Nunes Ferreira, Elad Nakar, Raquel Francisco, Mariana Pereira, Javier Moreno, Raphaël P Martins, Fausto J Pinto, João de Sousa

► **To cite this version:**

Gustavo Lima da Silva, Nuno Cortez-dias, Afonso Nunes Ferreira, Elad Nakar, Raquel Francisco, et al.. Impact of different activation wavefronts on ischemic myocardial scar electrophysiological properties during high-density ventricular tachycardia mapping and ablation. *Journal of Cardiovascular Electrophysiology*, 2022, 10.1111/jce.15740 . hal-03956186

**HAL Id: hal-03956186**

**<https://univ-rennes.hal.science/hal-03956186>**

Submitted on 25 Jan 2023

**HAL** is a multi-disciplinary open access archive for the deposit and dissemination of scientific research documents, whether they are published or not. The documents may come from teaching and research institutions in France or abroad, or from public or private research centers.

L'archive ouverte pluridisciplinaire **HAL**, est destinée au dépôt et à la diffusion de documents scientifiques de niveau recherche, publiés ou non, émanant des établissements d'enseignement et de recherche français ou étrangers, des laboratoires publics ou privés.



Distributed under a Creative Commons Attribution - NonCommercial - NoDerivatives 4.0 International License

# Impact of different activation wavefronts on ischemic myocardial scar electrophysiological properties during high-density ventricular tachycardia mapping and ablation

Gustavo Lima da Silva MD<sup>1,2</sup>  | Nuno Cortez-Dias MD, PhD<sup>1,2</sup>  |  
 Afonso Nunes Ferreira MD<sup>1,2</sup>  | Elad Nakar MsC<sup>3</sup> | Raquel Francisco MsC<sup>4</sup> |  
 Mariana Pereira MsC<sup>5</sup> | Javier Moreno MD, PhD<sup>6</sup> | Raphaël P. Martins MD, PhD<sup>7</sup>  |  
 Fausto J. Pinto MD, PhD<sup>1,2</sup> | João de Sousa MD<sup>1,2</sup>

<sup>1</sup>Cardiology Department, Santa Maria University Hospital (CHULN), Lisbon Academic Medical Centre, Lisbon, Portugal

<sup>2</sup>Cardiac Rhythm Abnormalities Unit, Cardiovascular Centre of the University of Lisbon, Lisbon School of Medicine of the Universidade de Lisboa, Lisbon, Portugal

<sup>3</sup>Research and Development Department, Biosense Webster, Johnson & Johnson, Yokneam, Israel

<sup>4</sup>Biosense Webster, Johnson & Johnson, EMEA Clinical Development, Diegem, Belgium

<sup>5</sup>Biosense Webster, Johnson & Johnson, Clinical Support, Porto Salvo, Portugal

<sup>6</sup>Cardiology Department, Arrhythmia Unit, University Hospital Ramón y Cajal and CIBER-CV Madrid, Madrid, Spain

<sup>7</sup>Department of Cardiology, Rennes University Hospital, Rennes, France

## Correspondence

Gustavo Lima da Silva, MD, Serviço de Cardiologia, Departamento de Coração e Vasos, CHULN Hospital de Santa Maria, Av Prof. Egas Moniz, 1649-028 Lisboa, Portugal. Email: [gustavossilva@gmail.com](mailto:gustavossilva@gmail.com)

## Abstract

**Introduction:** Scar-related ventricular tachycardia (VT) usually results from an underlying reentrant circuit facilitated by anatomical and functional barriers. The later are sensitive to the direction of ventricular activation wavefronts. We aim to evaluate the impact of different ventricular activation wavefronts on the functional electrophysiological properties of myocardial tissue.

**Methods:** Patients with ischemic heart disease referred for VT ablation underwent high-density mapping using Carto<sup>®</sup>3 (Biosense Webster). Maps were generated during sinus rhythm, right and left ventricular pacing, and analyzed using a new late potential map software, which allows to assess local conduction velocities and facilitates the delineation of intra-scar conduction corridors (ISCC); and for all stable VTs.

**Results:** In 16 patients, 31 high-resolution substrate maps from different ventricular activation wavefronts and 7 VT activation maps were obtained. Local abnormal ventricular activities (LAVAs) were found in VT isthmus, but also in noncritical areas. The VT isthmus was localized in areas of LAVAs overlapping surface between the different activation wavefronts. The deceleration zone location differed depending on activation wavefronts. Sixty-six percent of ISCCs were similarly identified in all activating wavefronts, but the one acting as VT isthmus was simultaneously identified in all activation wavefronts in all cases.

**Abbreviations:** DZ, deceleration zone; EGM, electrogram; ICD, implantable cardioverter-defibrillator; IHD, ischemic heart disease; ISCC, intra-scar conduction corridor; LAT, local activation time; LAR, late activation region; LAVA, local abnormal ventricular activity; LCV, local conduction velocity; LV, left ventricle; RV, right ventricle; SR, sinus rhythm; VT, ventricular tachycardia.

**Disclosures:** Nuno Cortez-Dias, João de Sousa, Javier Moreno, and Raphaël P. Martins have received travel and consulting fees from Biosense Webster, Boston Scientific, and Abbott Medical. Elad Nakar is an engineer used by Biosense Webster. Raquel Francisco and Mariana Pereira are Biosense Webster employees working as clinical specialists. The remaining authors declare no conflict of interest.

This is an open access article under the terms of the Creative Commons Attribution-NonCommercial-NoDerivs License, which permits use and distribution in any medium, provided the original work is properly cited, the use is non-commercial and no modifications or adaptations are made.

© 2022 The Authors. *Journal of Cardiovascular Electrophysiology* published by Wiley Periodicals LLC.

**Conclusion:** Functional based substrate mapping may improve the specificity to localize the most arrhythmogenic regions within the scar, making the use of different activation wavefronts unnecessary in most cases.

**KEYWORDS**

ablation, conduction velocity, mapping, ventricular tachycardia, wavefront

## 1 | INTRODUCTION

Scar-related monomorphic ventricular tachycardia (VT) in ischemic heart disease usually results from underlying reentrant circuits.<sup>1-3</sup> In hemodynamically stable VTs, activation and entrainment mapping can identify critical sites of the reentrant circuit that can be targeted for ablation. However, most VTs are not hemodynamically tolerated. As such, catheter ablation often depends on substrate-based treatment strategies, such as elimination of local abnormal ventricular activities (LAVA), representing regions of slowed conduction through scar.<sup>4</sup> These treatment strategies have shown to be superior to targeting only the clinical VTs and complete LAVA elimination was associated to improved arrhythmia free-survival.<sup>4-6</sup> Indeed, a recent meta-analysis found that there was a significantly lower risk of the primary composite outcome of VT recurrence or all-cause mortality among those undergoing a substrate-based ablation.<sup>7</sup>

Current substrate mapping strategies may lack sensitivity, as identification of LAVAs may be difficult when hidden within far-field signal.<sup>8</sup> Also, they may lack specificity, not distinguishing between arrhythmogenic scar regions (susceptible for reentry) from non-arrhythmogenic scar. Anter et al.,<sup>9</sup> in a swine model of myocardial infarction related VT reentry circuits and using ultra-high-density mapping technology found that the VT isthmus and critical zone correspond to zones with conduction velocity slowing during sinus rhythm (SR), with a positive predictive value of 60% and 70%, respectively. Although reentry is facilitated by anatomical barriers (fibrosis), its mere presence is insufficient and additional functional barriers are needed to produce the required electroanatomical milieu.<sup>10</sup> Importantly, these factors are sensitive to the direction of activation wavefronts. Arenal et al.<sup>11</sup> were the first to show vector-dependent recording of LAVAs. Furthermore, VT initiation is often dependent on premature beats interacting with the infarct from a specific direction and at a specific cycle length, thus producing local electrophysiological conditions that may not be present during SR. Therefore, a better understanding is needed of the associated variables that influence the generation of substrate maps.

This study aims to evaluate the impact of different ventricular activation wavefronts (SR, right ventricle [RV] or left ventricle [LV] pacing) on the electrophysiological properties of ischemic scar, focusing on local conduction velocity (LCV), and their correlation with the critical VT isthmus location.

## 2 | METHODS

### 2.1 | Study design and population

Between 2018 and June 2022, patients with a prior myocardial infarction and sustained monomorphic VT documented by surface electrocardiography or implantable cardioverter-defibrillator (ICD) referred for ablation at Santa Maria University Hospital were considered eligible for this study. The present analysis was restricted to patients with at least one of the following: (1) high-resolution LV substrate maps during different ventricular activation wavefronts using the Pentaray<sup>®</sup> mapping catheter and Carto<sup>®</sup>3 (Version 6 or 7; Biosense Webster, Inc.) before deployment of any radiofrequency energy; or (2) a detailed activation map during VT providing appropriate delineation of the critical isthmus, additionally proved by entrainment maneuvers and, if the VT was stable and tolerated, by termination with targeted radiofrequency application.

The Institutional Ethics Committee at our institution approved the collection and review of data. Prior written informed consent was obtained from all participants. Description of the electrophysiology procedure and workflows used for substrate map collection and VT activation mapping are presented as Supporting Information.

### 2.2 | Offline analyses

Maps were analyzed retrospectively using a noncommercial version of Carto<sup>®</sup>3 V8. The substrate map was analyzed using a new late potential map (LPM) software, which includes: a LAVA annotation algorithm; a localized bipolar voltage assessment; and an algorithm for automatic regional vector analysis, allowing to determine the directionality of the electrical wavefront and to display a quantitative assessment of LCV<sup>12</sup>—Supporting Information. Of note, localized bipolar voltage assessment allows automatic and dynamic adjustment of the window of interest focusing on the near-field signal and excluding any far-field component from the measurement. All electrograms (EGM) were reviewed by two operators (G. L. S. and N. C. D.) and a third reviewer (J. S.) gave his interpretation in case of discrepancies. Electronic callipers at similar gain of 0.20 mV/cm and speed of 200 mm/s were used during EGM analysis. The local activation time (LAT) annotation of multicomponent EGMs was defined using the method described by Anter et al.<sup>9</sup> which aims to

better differentiate near field from far field signals. The automatic annotation was accepted if it correctly annotated the near-field component. If the automatic algorithm failed to recognize the near-field signal, the annotation was manually corrected.

Areas of scar (defined as localized bipolar voltage  $<1.5$  mV) were delineated through adjustment of the voltage thresholds.<sup>13</sup> Border zone was defined as localized bipolar voltage 0.5–1.5 mV and dense scar as localized bipolar voltage  $<0.5$  mV. LAVAs were defined as a composite signal with at least a high-frequency potential clearly distinct from the far-field signal, occurring any time during or after the QRS complex.<sup>4</sup> This category included signals usually described as fractionated low-amplitude signals, split EGMs, and isolated late potentials<sup>9</sup>—Supplementary Figure 1. Activation maps were displayed as isochronal maps where the entire ventricular window was divided into eight isochrones. Deceleration zones (DZ) were defined by the presence of three colors within 1 cm.<sup>14</sup> Late activation regions (LAR) were defined as the area where the last 25% of the entire ventricular window was activated (dark blue and purple). LCV analysis was performed using a velocity cut-off of 0.20 mm/ms and a compression

level of 2. Intra-scar conduction corridors (ISCC) were defined as corridors of LCV vectors with: (1) LCV  $\leq 0.20$  mm/ms; (2) localized bipolar voltage  $<1.50$  mV; (3) length  $\geq 10$  mm; and (4) vector orientation parallel to the length of the corridor<sup>12</sup>—Figure 1. A novel propagation display of the LCV data superimposed on the activation maps was used to facilitate the delineation of the ISCC—Supplementary Movie 1. A slow conduction patch was defined as a site with LCV vectors  $<0.20$  mm/ms in a side-by-side parallel distribution.

High-resolution VT activation maps were reviewed, and all the EGMs were manually corrected to the near-field signals. The isthmus common channel was defined as the circuit portion bounded by two lateral lines of block or slow conduction, producing an orthodromic wavefront. The entrance region was defined as the site where the wavefront enters the isthmus common channel, and the exit as the site where the wavefront exits the common channel to activate the remainder ventricle. LCV during VT at the entrance region, common-channel, and exit region were assessed considering the following velocity cut-offs:  $\leq 0.10$ , 0.11–0.15, 0.16–0.20, and

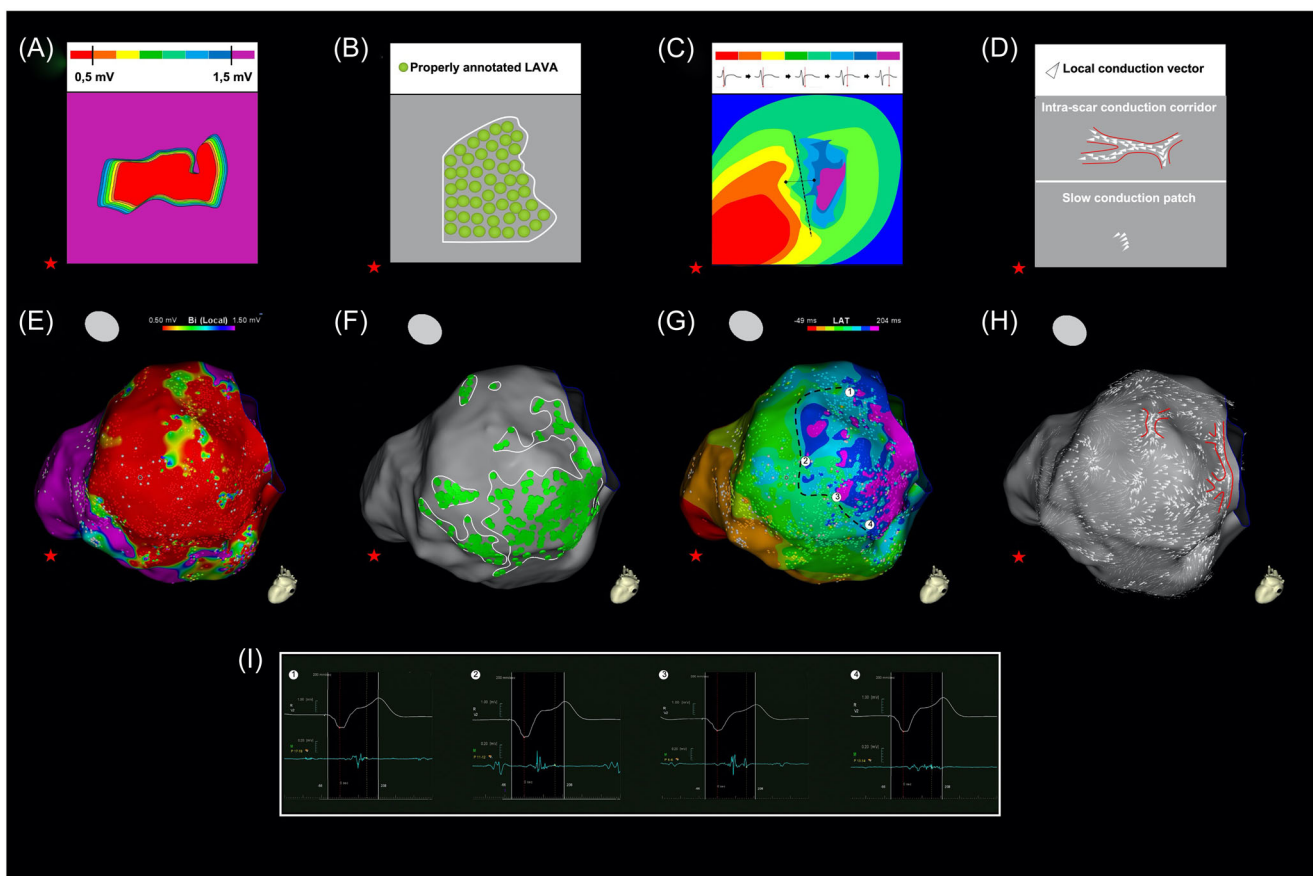


**FIGURE 1** Voltage, LAVAs, activation, and LCV maps during RV pacing in a patient with history of inferior and inferolateral wall infarction. (A) and (E) depict a schematic representation and an endocardial localized bipolar voltage map. (B) and (F) depict a schematic representation and an endocardial LAVAs map. (C) and (G) show a schematic representation and an endocardial activation map. A DZ (black dashed line) is defined by the presence of three colors within 1 cm where the entire ventricular window is divided into eight isochrones. (I) presents illustrative EGMs found in the DZ. (D) and (H) depict a schematic representation and an endocardial LCV map. Two ISCCs (within red lines) are depicted. Also note the wide distribution of slow conduction patches. DZ, deceleration zones; EGMs, electrogram; ISCC, intra-scar conduction corridors; LAVAs, local abnormal ventricular activities; LCV, local conduction velocities; RV, right ventricle.

>0.20 mm/ms. To evaluate the spatial concordance between the VT activation maps and substrate maps, VT isthmus dimensions were measured in terms of length, width, and surface area with respect to the portion of the common channel with LAT values corresponding to the 25%–75% VT diastolic interval. The VT isthmus orientation was considered longitudinal if it was parallel to the LV long axis (perpendicular to the mitral annulus plane) and circumferential if it was perpendicular to the LV long axis (parallel to the mitral annulus plane). SR and LV pacing activation wavefronts were considered perpendicular and parallel to longitudinal and circumferential VT isthmus, respectively; while RV pacing activation wavefront was considered parallel and perpendicular to longitudinal and circumferential VT isthmus, respectively—Supplementary Figure 2.

### 2.3 | Follow-up

Discontinuation of antiarrhythmic drugs and ICD programming were up to the discretion of the treating physician. ICDs were interrogated at each visit and through remote monitoring. Any documented monomorphic or polymorphic VT terminated by an appropriate ICD shock was considered a recurrence. Mortality during follow-up was categorized as either cardiovascular or non-cardiovascular.

### 2.4 | Statistical analysis

Continuous variables were described by the mean and SD for normally distributed data or median and IQR for non-normally distributed data. Categorical variables were expressed as counts or percentages. Comparisons of continuous data were performed using paired *t*-test. A *p* < .05 was considered statistically significant. All statistical analyses were performed using SPSS version 26.0 (IBM).

## 3 | RESULTS

### 3.1 | Population characteristics

Sixteen patients with ischemic VT were included. Table 1 and Supplementary Table 1 summarize their clinical characteristics. Most patients were male (*N* = 15), with a mean age of 65 ± 12 years. Mean time since myocardial infarction was 12 ± 10 years. Mean LV ejection fraction was 31 ± 9%. Based on preprocedural imaging, the ischemic scar was inferior/lateral in 9 and anterior/septal in the remaining 7 patients. All patients were on β-blockers, and 15 were on amiodarone. At least a high-density substrate map was collected before deployment of radiofrequency energy in all the 16 patients. In 7 patients, a detailed activation map during VT was obtained providing appropriate delineation of the critical isthmus. In 4 of such patients, VT was repeatedly recurring during substrate map collection making unfeasible to obtain substrate maps with different activation wavefronts, and a single complete substrate map was used for

analysis. In 9 patients with substrate maps collected under different activation wavefronts, the VT was non-sustained or non-tolerated, rendering the VT activation maps incomplete and unsuitable for detailed comparison.

**TABLE 1** Baseline characteristics of the patients

Patient characteristics <sup>a</sup>	<i>N</i> = 16
Age (year)	65 ± 12
Male sex—no (%)	15 (94)
Ischemic heart disease	
Time since last myocardial infarction—year	12 ± 10
Previous percutaneous revascularization—no (%)	12 (75)
Previous surgical revascularization—no (%)	3 (19)
Heart failure and comorbidities	
NYHA functional class	
I/II—no (%)	3 (19)/10 (62)
II—no (%)	3 (19)
LV ejection fraction (%)	31 ± 9
Hypertension—no (%)	15 (94)
Diabetes—no (%)	6 (38)
Renal failure <sup>b</sup> —no (%)	6 (38)
Estimated GFR <sup>c</sup>	67 ± 27
Cardiovascular medication	
Antiarrhythmic drug—no (%)	15 (94)
Amiodarone—no (%)	15 (94)
Beta-blocker—no (%)	16 (100)
ICD device	
Indication for ICD before the index procedure—no (%)	14 (88)
Primary prevention—no (%)	8 (50)
Secondary prevention—no (%)	6 (38)
ICD implanted after index procedure—no (%)	2 (12)
Previous VT ablation—no (%)	2 (12)
Indication for ablation	
Sustained VT requiring external cardioversion—no (%)	7 (44)
Appropriate ICD shock—no (%)	9 (56)
VT storm—no (%)	4 (25)

Abbreviations: GER, glomerular filtration rate; ICD, Implantable cardioverter defibrillator; LV, left ventricle; NYHA, New York Heart Association; VT, ventricular tachycardia.

<sup>a</sup>Plus-minus values are means ± SD.

<sup>b</sup>Estimated GFR ≤60 ml/m<sup>2</sup>.

<sup>c</sup>The estimated GFR was calculated with the use of the Cockcroft–Gault formula.

### 3.2 | Impact of different activation wavefronts on the substrate map

To explore the impact of the different ventricular activation wavefronts on the electrophysiological properties of ischemic scar, we analyzed data from the patients in whom several substrate maps were possible to complete. In such 12 patients, 27 high-resolution LV substrate maps were obtained in: 6 in SR, 12 in RV pacing, and 9 in LV pacing—Supplementary Table 2. The mean  $\pm$  SD number of different activation wavefronts per patient was  $2.3 \pm 0.5$ . SR maps were not possible to obtain in 6 patients with atrioventricular block or permanent atrial fibrillation and LV paced maps were not obtained in 3 patients because a suitable lateral branch of the coronary sinus could not be cannulated. Complete LV maps were made in each case to allow accurate comparisons, with a mapped chamber surface area of  $188 \text{ cm}^2$  (IQR: 139–229). Maps comprised a total of 70 642 EGMs ( $2530 \pm 1166$  per map), of which 8051 (11.4%) were classified as LAVAs ( $298 \pm 173$  per map). Point density at scar regions was 27 points/ $\text{cm}^2$  (IQR: 12–46) and at normal areas was 5 points/ $\text{cm}^2$  (IQR: 2–6). There were no significant differences between maps with different directions of activation wavefront regarding the mapped chamber surface area, total number of EGMs, or number of LAVAs—Supplementary Table 3.

#### 3.2.1 | Localized bipolar voltage

Scar, as assessed based on localized bipolar voltage, was present in  $100.2 \text{ cm}^2$  (IQR: 83.5–110.3), representing  $54 \pm 14\%$  of the total LV chamber surface area. Scar area did not differ significantly in respect to the direction of wavefront activation—Figure 2 and Supplementary Table 3.

#### 3.2.2 | LAVAs distribution

LAVAs were present in  $10.1 \text{ cm}^2$  (IQR: 6.5–18.6), representing  $8 \pm 5\%$  of the total LV chamber surface area. Regarding the direction of wavefront activation, there was a trend for larger LAVAs area with RV pacing, but the difference was not statistically significant—Supplementary Table 3. LAVAs spatial concordance between (1) SR and RV maps was  $42.8 \pm 3.7\%$  ( $N = 6$ ); (2) RV pacing and LV maps was  $41.4 \pm 4.9.1\%$  ( $N = 9$ ); (3) SR and LV maps was  $42.3 \pm 6.1\%$  ( $N = 3$ ); (4) SR, RV, and LV maps was  $33.3 \pm 1.5\%$  ( $N = 3$ )—Figure 2. LAVAs were observed at dense scar regions in all the maps and were also present in the scar border zone in 15 (56%), while only 1 map presented LAVAs in the myocardium with normal localized bipolar voltage. Additionally, LAVAs were present in DZ and LAR in all substrate maps, independently of the direction of wavefront activations. However, they were also found in non-DZ and in the mid-50% activated regions in all maps and in the early-25% activated regions in 5 maps (19%). LAVAs were also observed at ISCCs in all substrate maps, independently

of the direction of wavefront activations, although they were also found in non-corridor areas in all the maps.

#### 3.2.3 | Activation pattern

All substrate maps presented at least one DZ, which resulted in LAR. However, DZ location per patient and subsequent LAR was different and dependent on the activation wavefront direction. Both DZ and LAR laid in dense scar in all maps and extended to the scar border zone in 4 cases (15%), while they were not found in areas of normal localized bipolar voltage. Additionally, LAR corresponded to areas with LAVAs in all maps, regardless of the different activating wavefront—Figure 2.

#### 3.2.4 | LCV analysis

LCV analysis in high-density substrate maps identified a median of three ISCCs per map (IQR: 2–3)—Figure 2. The number of ISCCs did not differ significantly when comparing different directions of wavefront activation—Supplementary Table 3. Most maps had ISCCs with multiple entries ( $n = 25$ ; 93%) and the majority (60%) of ISCCs had multiple entries. Additionally, most maps had interconnected channels ( $n = 18$ ; 67%). ISCCs laid in dense scar in all maps and extended to the scar border zone in 13 maps (48%). Additionally, ISCCs corresponded to areas with LAVAs in all maps. All substrate maps presented at least one ISCC at the LAR, but ISCCs were also found at the mid-50% activated regions in 24 maps (89%) and at the early-25% activated regions in 8 (30%) maps. Finally, slow conduction patches, composed of slow velocity vectors in a side-by-side distribution, not forming channels, were seen at the outer border zone of the scar in all substrate maps.

In a per patient analysis, a median of 3.5 ISCCs were identified (IQR: 3–4). Sixty-six percent of ISCCs were similarly identified in all available activation wavefronts per patient.

### 3.3 | VT circuit topography

VT activation maps providing appropriate delineation of the isthmus common channel were available in 7 patients (1 VT mapped per patient;  $3005 \pm 2033$  points per map). Detailed substrate maps created from one activation wavefront were available for comparison in 4 of them, and from two different wavefronts in 3—Supplementary Table 2.

Mean QRS duration was  $184 \pm 19$  ms and tachycardia cycle length was  $475 \pm 76$  ms (range: 378–597 ms). The macro-reentrant circuit comprised a dual-loop mechanism in 5 patients, a single-loop mechanism in 1, patient and a triple-loop mechanism (implying an inner-loop) in the remaining patient. Activation maps demonstrated reentrant circuits with a variety of isthmus morphologies, with a median VT isthmus length, width, and area of 31 mm (IQR: 23–39),

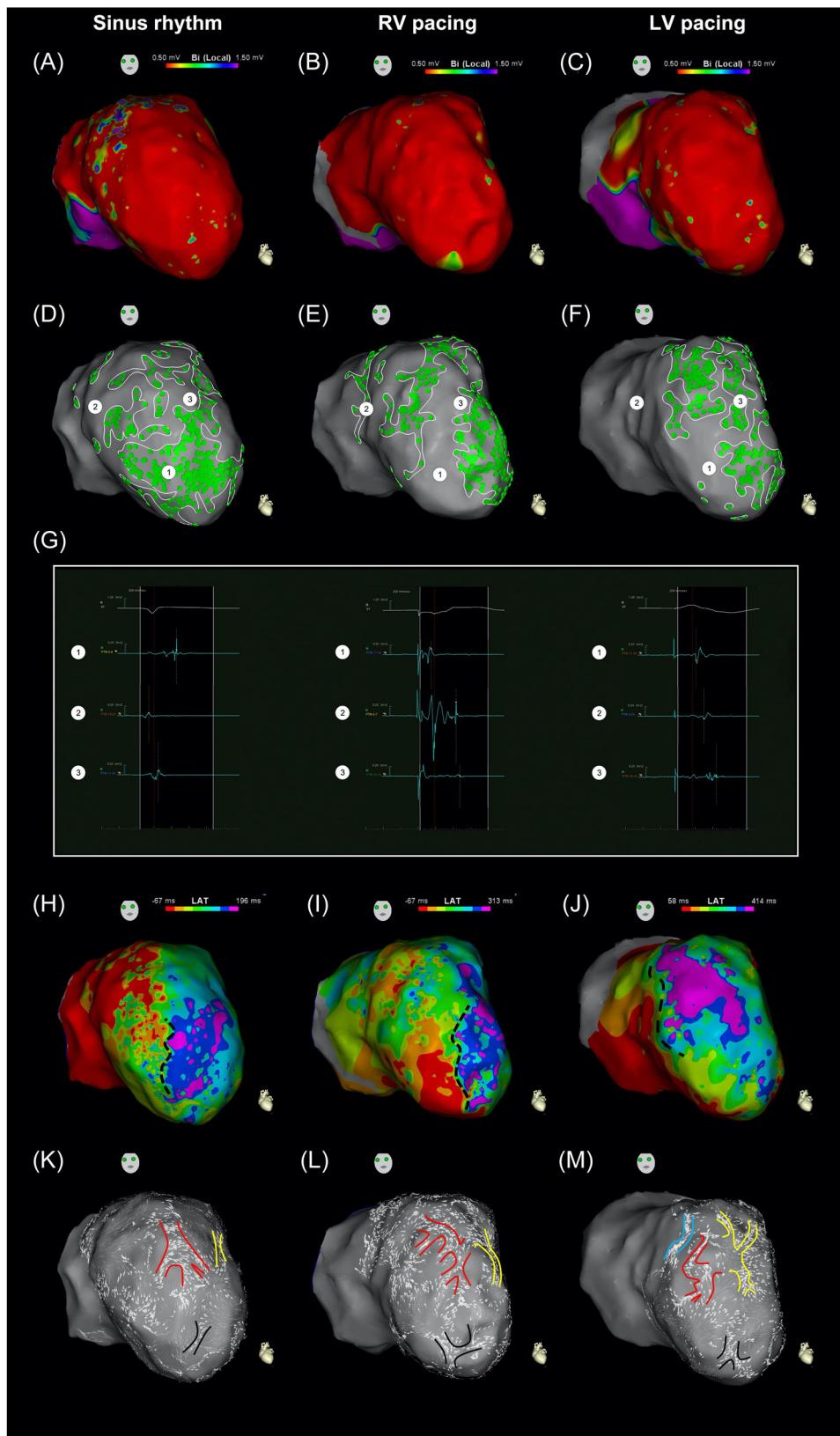


**FIGURE 2** (See caption on next page)

11 mm (IQR: 10–19), and 6.3 cm<sup>2</sup> (IQR: 5.2–8.6), respectively. All VT maps presented at least one portion of the VT isthmus with LCV  $\leq 0.20$  mm/msec. Within the VT isthmus, the slowest region varied: in 5 patients (71%) it was the entrance region; in 1 it was the exit region; and the remaining patient presented LCV equally slow at the common-channel/exit—Supplementary Table 4. For anterior/septal scar (3 out of 7), the VT isthmus was longitudinal in its main axis in 2 patients and circumferential in 1 patient; while for inferior/lateral scar (4 out of 7), the VT isthmus was circumferential in all 4.

### 3.4 | Relation between VT activation map and substrate map

In the 4 patients in whom the substrate map was available with one activation wavefront, 3 had an inferior/lateral scar and the remaining patient had an anterior/septal scar. In all 4 patients the VT isthmus axis was circumferential. The substrate map was acquired during SR in 3 patients, hence mostly parallel to the VT isthmus axis; and during RV pacing in the remaining patient, hence mostly perpendicular to the VT isthmus axis. The localized bipolar voltage amplitude at VT isthmus sites was consistently  $\leq 0.5$  mV in all cases. There was also a strong relationship between the location of the VT isthmus and LAVAs, with all maps presenting LAVAs at the isthmus site, although a mean of  $44 \pm 20\%$  of its area was not covered by LAVAs. However, localized bipolar voltage  $\leq 0.5$  mV and LAVAs were also found in noncritical areas (i.e., outer loops) in all maps. The region of VT isthmuses laid within DZ and mid-50% activating regions or LAR in all cases. LCV analysis in high-density substrate maps identified a mean of  $3 \pm 1$  ISCCs per patient, including the 1 acting as VT isthmus in all cases—Figure 3. Three out of 4 patients had channels with multiple entries.

On the other hand, in the 3 additional patients where the substrate map was available with two activation wavefronts, 2 had anterior/septal scar and the remaining patient had an inferior/lateral scar. In the two anterior/septal scar patients the VT isthmus axis was longitudinal, and in the inferior/lateral scar patient the VT isthmus axis was circumferential. In all 3 patients there was one parallel and one perpendicular activation wavefront to the VT isthmus axis. The localized bipolar voltage amplitude at VT isthmus sites was consistently  $\leq 0.5$  mV with both parallel and perpendicular activation.

LAVAs were found at the VT isthmus sites with both wavefronts. However, the proportion of the VT isthmus not covered by LAVAs was significantly smaller with parallel versus perpendicular wavefront activation ( $N = 3$ ,  $21 \pm 10$  vs.  $26 \pm 11\%$ ,  $p = .03$ )—Figure 4. Additionally, the VT isthmus was localized in areas of LAVAs overlapping surface between the available wavefronts. The region of VT isthmuses laid within DZ and mid-50% activating regions or LAR, regardless of the pacing wavefront. LCV analysis identified 3 ISCCs in each patient. Seventy-eight percent of ISCCs were similarly identified in all available activating wavefronts per patient. Of notice, the ISCC acting as the VT isthmus was identified in both activation wavefronts in all cases.

### 3.5 | Outcome

In the 7 patients where the clinical VT was mapped, VT was non-inducible at the end of the procedure. LAVAs were successfully eliminated in 15 of the 16 cases. Procedural time was  $307 \pm 56$  min and total radiofrequency time was  $53 \pm 21$  min. Vascular access complications occurred in 2 patients, without further acute adverse events. During a mean follow up of  $22 \pm 19$  months, 2 patients had VT recurrence and 3 patients died: 2 due to end-stage heart failure related-events and 1 due to septic shock.

## 4 | DISCUSSION

The major findings of this study were:

1. Although LAVAs were predominantly found in dense scar regions, DZ, LAR, and ISCCs, they were also found in additional areas in a large proportion of maps, regardless of the activation wavefront. The overlap of LAVAs surface area between different activation wavefronts is low.
2. The DZ location differed depending on activation wavefronts. However, 66% of ISCCs were similarly identified in all available activating wavefronts per patient.
3. LAVAs were always present at the VT isthmus location, but also in noncritical areas. The proportion of the VT isthmus not covered by LAVAs was significantly smaller with parallel versus

**FIGURE 2** Spatial distribution of voltage, LAVAs, activation, and LCV under different directions of LV activation wavefront in a patient with history of anterior wall infarction and an apical aneurism. (A–C) Localized bipolar scar areas did not significantly differ dependent on the direction of wavefront activation and a large dense scar core was found. (D–F) LAVAs distribution is large and extremely heterogeneous, resulting in a LAVAs spatial concordance between the three pacing wavefronts of 33%. (G) presents illustrative EGMs found in areas where LAVAs are present with one wavefront but not with the other two. (H–J) A DZ (black dashed line) was found in each activation wavefront. The general area of activation slowing was different and dependent on the activation wavefront direction. (K–M) LCV map depicting ISCCs in each activation wavefront. Notice: (1) the similar general anatomical distribution of the ISCCs within red, yellow, and black lines in each activation wavefront although with different multiple entries, (2) One ISCC within blue lines was only found in LV pacing. DZ, deceleration zones; EGMs, electrogram; ISCC, intra-scar conduction corridors; LAVAs, local abnormal ventricular activities; LCV, local conduction velocities; LV, left ventricle.

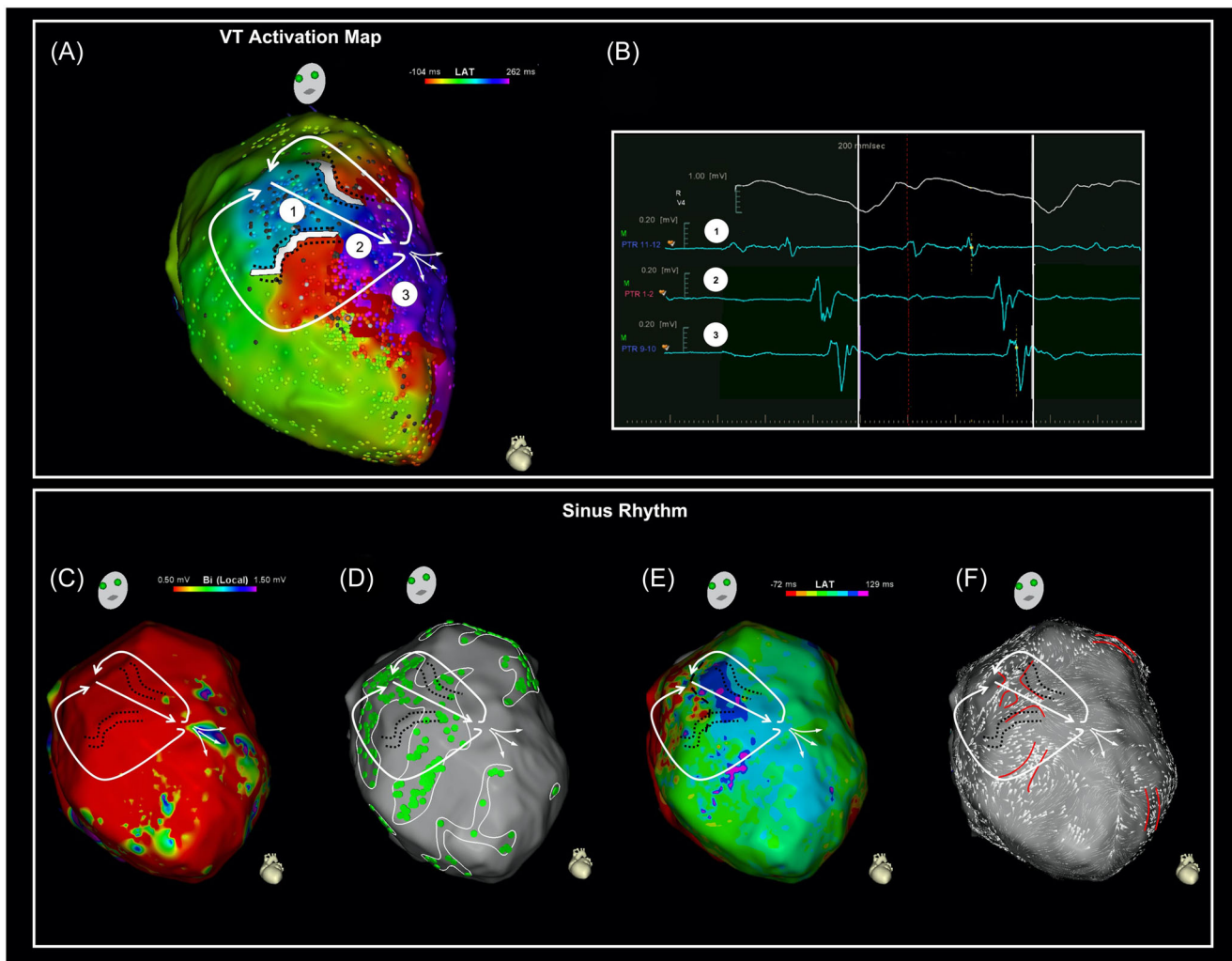


**FIGURE 3** Relationship between VT isthmus location and substrate maps in a patient with a history of anterior wall infarction and an apical aneurism. (A) VT activation map, TCL 378 ms, demonstrating a dual-loop mechanism, with a circumferential VT isthmus. (B) Presents illustrative late-diastolic EGMs found within the VT isthmus. Substrate maps were collected with SR, hence mostly parallel to the VT isthmus. (C) The VT isthmus is located within dense scar area. (D) Although there is a strong relationship between the location of the VT isthmus and LAVAs, the latter are also found in noncritical areas (i.e., outer loops). (E) A DZ (black dashed lines) transects the VT isthmus. (F) Four ISCCs were present, including the one acting as the VT isthmus. DZ, deceleration zones; EGMs, electrogram; ISCC, intra-scar conduction corridors; LAVAs, local abnormal ventricular activities; SR, sinus rhythm; VT, ventricular tachycardia.

perpendicular wavefront activation. The VT isthmus was localized in areas of LAVAs overlapping surface between the available wavefronts.

- The ISCC acting as the VT isthmus was similarly identified in the substrate maps created with the several activation wavefronts in all the cases.

Significant differences in scar and LAVAs characterization with different activation wavefronts were first demonstrated by Arenal et al.<sup>11</sup> Tung et al.<sup>15</sup> have investigated the impact of the activation wavefront direction on the values obtained during voltage mapping. Significant differences in bipolar and unipolar low-voltage characterization of scar with different ventricular activation wavefronts were observed, mainly in septal locations and in patients with

heterogeneous scar. They concluded that an alternate activation wavefront increased the sensitivity to detect arrhythmogenic substrate and critical areas for VT. However, major limitations of such study were the use of a 3.5 mm irrigated tip ablation catheters for mapping in most patients and the use of non-localized bipolar voltage assessment (with a fixed window of interest, that necessarily includes the far-field signal which usually has higher voltage than LAVAs, thus distorting the measurements). Both increase the far-field recording and reduce accuracy in comparison with multipolar catheters with short interelectrode spacing and localized bipolar voltage.<sup>16,17</sup> Martin et al.,<sup>18</sup> using the ultra-high-density Rhythmia<sup>®</sup> system, with the 64-electrode minibasket Orion<sup>®</sup> mapping catheter (Boston Scientific) demonstrated that RV and LV pacing resulted in smaller non-localized bipolar scar area than with SR. In our study,

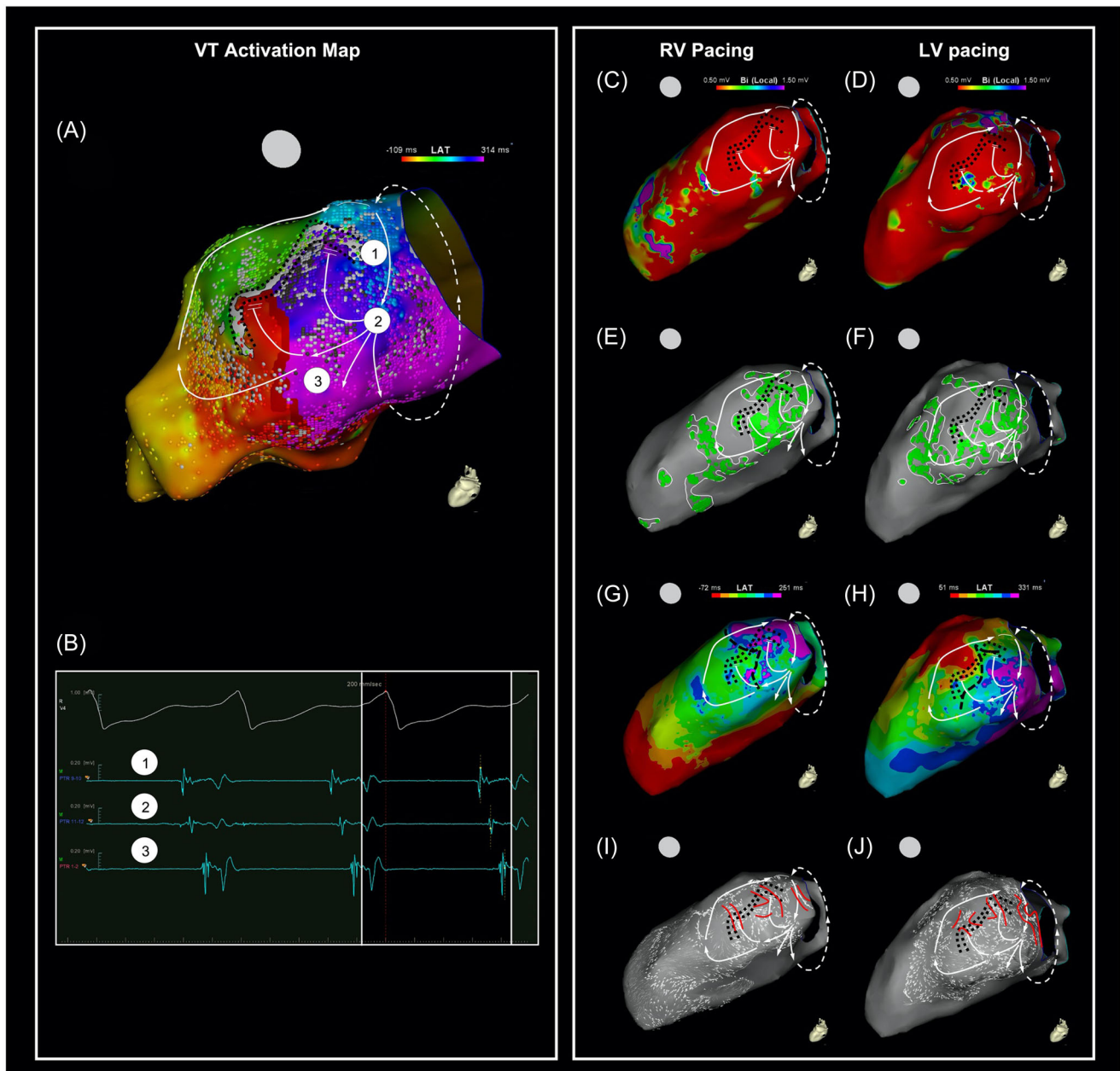


**FIGURE 4** Relationship between VT isthmus location and substrate maps under different LV activation wavefronts in a patient with a history of inferior and inferolateral wall infarction. (A) VT activation map, TCL 536 ms, demonstrating a dual-loop mechanism, with a circumferential VT isthmus. (B) Presents illustrative late-diastolic EGMs found within the VT isthmus. Substrate maps were collected with RV and LV pacing, hence mostly perpendicular and parallel to the VT isthmus, respectively. (C, D) The VT isthmus is located within dense scar area in both RV and LV pacing wavefronts. (E, F) Although there is a strong relationship between the location of the VT isthmus and LAVAs in both RV and LV pacing wavefronts, the latter are also found in noncritical areas (i.e., outer loops). (G, H) DZ (black dashed lines) transect the VT isthmus in both RV and LV pacing wavefronts, although the area of activation slowing was different and dependent on the activation wavefront direction. (I, J) Three ISCCs were found in both RV and LV pacing wavefronts. Notice that in both wavefronts, one acts as the VT isthmus and the other two correspond to dead-ends during VT. DZ, deceleration zones; EGMs, electrogram; ISCC, intra-scar conduction corridors; LAVAs, local abnormal ventricular activities; LV, left ventricle; RV, right ventricle; VT, ventricular tachycardia.

using the high-density Carto<sup>®</sup>3 system, with the 20-electrode Pentaray<sup>®</sup> mapping catheter and localized bipolar voltage assessment (automatic and dynamic adjustment of the window of interest focusing on the near-field signal and excluding any far-field component from the measurement), scar areas did not differ

significantly when using different directions of wavefront activation. Such discrepancy regarding prior studies allows to hypothesize that the voltage differences previously reported might have been largely influenced by the far-field contribution to the overall EGM voltage. Since this novel localized bipolar voltage assessment was found to be

consistent and independent of the activation wavefront, it may eventually reduce the need for assessing the substrate properties under alternative wavefronts.

Of note, signal characteristics seem more important than voltage alone. LAVAs timing may be affected by their location, and the chance of detecting LAVAs increases when EGM onset is later relative to the QRS complex. As such, mapping with a pacing wavefront which allows separation of the QRS from the LAVAs signal improves LAVAs characterization. Martin et al.,<sup>18</sup> showed that RV and LV pacing resulted in larger LAVAs surface area than with SR. We observed a trend for larger LAVAs surface area using RV pacing. Anter et al.<sup>9</sup> previously demonstrated that LAVAs have a high sensitivity but a poor specificity for the VT isthmus, having a negative predictive value of 96%. This means that LAVAs may be found in noncritical areas, which is consistent with our observations. Additionally, we found that the VT isthmus was localized in areas of LAVAs overlapping surface between the available wavefronts, which means that the VT isthmus would not be missed using a single activation wavefront.

Isthmuses of different VTs often share a common region, which can be identified during SR as an area with steep conduction slowing.<sup>9</sup> Isochronal crowding regions during the baseline rhythm were predictive of VT termination sites, providing mechanistic evidence that DZ are highly arrhythmogenic, and result in a more targeted substrate-based ablation approach, obviating the need for extensive radiofrequency delivery.<sup>19</sup> We found that VT isthmus laid within dense scar, in DZ and mid-50% activating regions or LAR. However, DZ location differed depending on activation wavefronts. Such visual analysis completely depends on the operator's experience and may be challenging, namely if the areas displaying activation slowing are located close to the source of LV activation or are activated during the QRS complex, since the spatial distribution of activation slowing depends on the direction of LV activation.<sup>20</sup> Despite this, selective ablation in cumulative areas of slow activation during activation from multiple directions proved to be successful.<sup>20</sup>

In this study, we explore the use of LCV data to assist the delineation of regions of interest and the identification of targets for ablation. The identification of the ISCC was purely based on the analysis of LCV vectors, using simple criteria recently proposed by our group.<sup>12</sup> Additionally, we used for the first time a novel propagation display of the LCV data superimposed on the activation maps, as shown in Supplementary Movie 1, which made the delineation of ISCC much easier. In the current study, we found that 66% of ISCCs were similarly identified in all available activating wavefronts per patient. Importantly, the ISCC acting as the VT isthmus was identified in all available wavefronts in all cases. As such, LCV analysis may improve the specificity of localizing the most arrhythmogenic regions within the scar and reduce the need to characterize the substrate properties under different activation wavefronts.

Performing entire substrate maps with SR, RV, and LV pacing is time-consuming. Nevertheless, with multipolar catheters and automatic annotation algorithms, serial mapping is becoming faster and

feasible. In addition, multiple substrate maps of the entire LV are unnecessary. In specific cases, if the initial map demonstrates an area of scar with a paucity of LAVAs, additional mapping with alternative wavefronts could be confined to that region.

The major limitation of this study is being a single center non-prospective study with few patients. Furthermore, only a small number of VT circuits were tolerated to allow detailed mapping. Additionally, the retrospective use of the LPM software might have underestimated its potential. A prospective multicenter study in now recruiting patients to further explore and validate the use of the LPM algorithm for substrate characterization in patients undergoing VT ablation. The scar dimensions in the maps were determined using the bipolar voltage thresholds of 0.5–1.5 mV and no differences were found in relation to the activation wavefront. In the era of high-density mapping based on catheters with small electrodes and reduced interelectrode spacing, there is an unmet need for reassessing these thresholds, and much lower values seem to be appropriate for channel delineation. However, since no standardized values have been presented so far, we opted to keep the conventional values, facilitating the comparison of our results with prior studies. Finally, functional properties of the substrate were not explored using provocative maneuvers such as Decrement-Evoked Potential mapping with extra stimulus.<sup>21</sup>

## 5 | CONCLUSION

Functional based substrate mapping characterization may improve the specificity to localize the most arrhythmogenic regions within the scar, making the use of different activation wavefronts unnecessary in most cases.

### DATA AVAILABILITY STATEMENT

The data generated during and/or analyzed during the current study are available from the corresponding author on reasonable request.

### ORCID

Gustavo Lima da Silva  <http://orcid.org/0000-0003-3138-8354>

Nuno Cortez-Dias  <http://orcid.org/0000-0002-9244-4631>

Afonso Nunes Ferreira  <http://orcid.org/0000-0002-2836-9497>

Raphaël P. Martins  <http://orcid.org/0000-0001-5716-6712>

### REFERENCES

1. Martin R, Maury P, Biscaglia C, et al. Characteristics of scar-related ventricular tachycardia circuits using ultra-high-density mapping. *Circ Arrhythm Electrophysiol*. 2018;11:e006569.
2. Tung R, Raiman M, Liao H, et al. Simultaneous endocardial and epicardial delineation of 3D reentrant ventricular tachycardia. *J Am Coll Cardiol*. 2020;75:884-97.
3. Nishimura T, Upadhyay GA, Aziz ZA, et al. Circuit determinants of ventricular tachycardia cycle length. *Circulation*. 2021;143:212-26.
4. Jaïs P, Maury P, Khairy P, et al. Elimination of local abnormal ventricular activities: a new end point for substrate modification in patients with scar-related ventricular tachycardia. *Circulation*. 2012;125:2184-2196.

5. Di Biase L, Burkhardt JD, Lakkireddy D, et al. Ablation of stable VTs versus substrate ablation in ischemic cardiomyopathy. *J Am Coll Cardiol*. 2015;66:2872-82.
6. Wolf M, Sacher F, Cochet H, et al. Long-term outcome of substrate modification in ablation of post-myocardial infarction ventricular tachycardia. *Circ: Arrhythm Electrophysiol*. 2018;11:e005635.
7. Briceño DF, Romero J, Villablanca PA, et al. Long-term outcomes of different ablation strategies for ventricular tachycardia in patients with structural heart disease: systematic review and meta-analysis. *EP Europace*. 2018;20:104-115.
8. Komatsu Y, Daly M, Sacher F, et al. Electrophysiologic characterization of local abnormal ventricular activities in postinfarction ventricular tachycardia with respect to their anatomic location. *Heart Rhythm*. 2013;10:1630-1637.
9. Anter E, Kleber AG, Rottmann M, et al. Infarct-related ventricular tachycardia. *JACC: Clin Electrophysiol*. 2018;4:1033-1048.
10. Josephson ME, Anter E. Substrate mapping for ventricular tachycardia. *JACC: Clin Electrophysiol*. 2015;1:341-352.
11. Arenal A, Glez-Torrecilla E, Ortiz M, et al. Ablation of electrograms with an isolated, delayed component as treatment of unmappable monomorphic ventricular tachycardias in patients with structural heart disease. *J Am Coll Cardiol*. 2003;41:81-92.
12. Cortez-Dias N, Lima da Silva G, Nunes-Ferreira A, et al. Novel "late potential map" algorithm: abnormal potentials and scar channels detection for ventricular tachycardia ablation. *J Cardiovasc Electrophysiol*. 2022;33:1211-1222.
13. Marchlinski FE, Callans DJ, Gottlieb CD, Zado E. Linear ablation lesions for control of unmappable ventricular tachycardia in patients with ischemic and nonischemic cardiomyopathy. *Circulation*. 2000;101:1288-1296.
14. Raiman M, Tung R. Automated isochronal late activation mapping to identify deceleration zones: rationale and methodology of a practical electroanatomic mapping approach for ventricular tachycardia ablation. *Comput Biol Med*. 2018;102:336-40.
15. Tung R, Josephson ME, Bradfield JS, Shivkumar K. Directional influences of ventricular activation on myocardial scar characterization: voltage mapping with multiple wavefronts during ventricular tachycardia ablation. *Circ: Arrhythm Electrophysiol*. 2016;9:e004155.
16. Tschabrunn CM, Roujol S, Dorman NC, Nezafat R, Josephson ME, Anter E. High-resolution mapping of ventricular scar: comparison between single and multielectrode catheters. *Circ: Arrhythm Electrophysiol*. 2016;9:e003841.
17. Berte B, Relan J, Sacher F, et al. Impact of electrode type on mapping of scar-related VT. *J Cardiovasc Electrophysiol*. 2015;26:1213-1223.
18. Martin CA, Martin R, Maury P, et al. Effect of activation wavefront on electrogram characteristics during ventricular tachycardia ablation. *Circ: Arrhythm Electrophysiol*. 2019;12:e007293.
19. Aziz Z, Shatz D, Raiman M, et al. Targeted ablation of ventricular tachycardia guided by wavefront discontinuities during sinus rhythm: a new functional substrate mapping strategy. *Circulation*. 2019;140:1383-1397.
20. Anter E, Neuzil P, Reddy VY, et al. Ablation of reentry-vulnerable zones determined by left ventricular activation from multiple directions: a novel approach for ventricular tachycardia ablation: a multicenter study (PHYSIO-VT). *Circ: Arrhythm Electrophysiol*. 2020;13:e008625.
21. Porta-Sánchez A, Jackson N, Lukac P, et al. Multicenter study of ischemic ventricular tachycardia ablation with decrement-evoked potential (DEEP) mapping with extra stimulus. *JACC: Clin Electrophysiol*. 2018;4:307-315.

## SUPPORTING INFORMATION

Additional supporting information can be found online in the Supporting Information section at the end of this article.

**How to cite this article:** Lima da Silva G, Cortez-Dias N, Nunes Ferreira A, et al. Impact of different activation wavefronts on ischemic myocardial scar electrophysiological properties during high-density ventricular tachycardia mapping and ablation. *J Cardiovasc Electrophysiol*. 2022;1-11. doi:10.1111/jce.15740